RESEARCH ARTICLE SUMMARY

OCEAN CARBON

Antarctic krill vertical migrations modulate seasonal carbon export

A. J. R. Smith*, S. Wotherspoon, L. Ratnarajah, G. R. Cutter, G. J. Macaulay, B. Hutton, R. King, S. Kawaguchi, M. J. Cox

INTRODUCTION: Antarctic krill (*Euphausia superba*) is among the most abundant animals on the planet (between 117 and 379 million tonnes). Krill play a vital role in the biological carbon pump—a biologically driven mechanism that sequesters carbon to the deep ocean—by consuming phytoplankton in the upper water column and producing fast-sinking fecal pellets which sink to the seafloor. Sinking particles, including carbon-rich fecal pellets, are vulnerable to degradation through fragmentation, reingestion, dissolution into the surrounding seawater, or bacterial remineralization. This means that not all of the material consumed by krill in the upper ocean is exported to deeper depths, and some of the consumed carbon is returned to the upper ocean. Vertical migration, a behavior common to krill and many zooplankton and fish species worldwide, is believed to increase the efficiency of the biological carbon pump by actively transporting particulate organic carbon consumed by organisms in the upper ocean directly into the mesopelagic zone (waters deeper than 200 m) with minimal degradation.

RATIONALE: Active acoustic techniques using ship-based echosounders are commonly used to observe vertical migration patterns. However, when observing krill and zooplankton, sound attenuation restricts these observations to the upper 250 m of the water column. Moreover, impenetrable Antarctic sea ice prevents access by ships to important krill habitats in winter, limiting the seasonal resolution of vertical migration observations. A lack of observational data means that few global climate models include vertical migration as a mechanism for carbon export or models rely on broad assumptions with little exploration into seasonal variability. The exclusion of vertical migrations has been suggested to have considerable influence on the accuracy of carbon export estimates by global climate models. Using echosounder observations from a seafloor lander in East Antarctica coupled with a numerical model, we explore how observed patterns in vertically migrating krill contribute to the total particulate organic carbon flux across a full year.

Lights, camera, krill. East Antarctic mooring reveals hidden behavior of Antarctic krill on the seafloor with acoustic observations used to explore year-round vertical migration patterns and particulate organic carbon sequestration by this important species.

RESULTS: An upward-looking echosounder positioned at 385-m depth on the continental shelf of Prydz Bay provided full water column high-resolution observations of krill density and depth every 7 min for a full year. Video camera footage captured Antarctic krill swarming around lights on the lander close to the seafloor with fecal pellets produced at depth. Over the year of observations, one-quarter of the krill population participated in vertical migrations between shallower epipelagic waters (<200 m) into deeper mesopelagic waters (>200 m). Krill were observed to typically complete one full cycle of vertical migration per day, and the amplitude of these migrations were highly seasonal. In summer, vertical migrations were restricted to the upper 100 m, giving krill an opportunity to graze on the phytoplankton. The greatest fraction of krill migrating into mesopelagic waters occurred in winter (when surface primary productivity was lowest), where krill performed full water column migrations from the surface to the seabed. Consequently, nonmigrating krill exported 8.4 mg C m^{-2} day^{-1} from sinking fecal pellets released in the upper water column, whereas migrating krill injected considerably less particulate organic carbon (1.3 mg C m^{-2} day^{-1}) into the mesopelagic zone over a full year. Carbon injection by migrating krill was highly seasonal, with the largest contributions to carbon flux in winter (when a greater proportion of migrating krill were present), but overall vertical migration contributed less than 10% of the total krill particulate organic carbon flux.

CONCLUSION: Our observations show high seasonal variability in krill diel vertical migration patterns with almost no migration occurring into the mesopelagic during summer. Modeling results suggest that previous estimates of carbon injection by migrating krill, which are based on assumed rather than observed vertical migration behavior, have been overestimated and that the Antarctic krill migrant pump has a minor contribution to particulate organic carbon export. This contradicts established theories on the value of vertical migration to the biological carbon pump. However, increased attention is required to resolve changes to krill grazing behaviors and attenuation processes such as bacterial remineralization that are likely to affect carbon export and potentially influence the effect of vertical migration on the downward flux of carbon to deep waters. ■

The list of author affiliations is available in the full article online.
*Corresponding author. Email: abigail.smith@utas.edu.au
Cite this article as A. J. R. Smith *et al.*, *Science* **387**, eadq5564 (2025). DOI: 10.1126/science.adq5564

READ THE FULL ARTICLE AT
https://doi.org/10.1126/science.adq5564

RESEARCH ARTICLE

OCEAN CARBON

Antarctic krill vertical migrations modulate seasonal carbon export

A. J. R. Smith[1,2]*, S. Wotherspoon[2], L. Ratnarajah[1], G. R. Cutter[3], G. J. Macaulay[4], B. Hutton[5], R. King[2], S. Kawaguchi[1,2], M. J. Cox[1,2]

Vertical migrations by marine organisms contribute to carbon export by consumption of surface phytoplankton followed by defecation in the deep ocean. However, biogeochemical models lack observational data, leading to oversimplified representation of carbon cycling by migrating organisms, such as Antarctic krill (*Euphausia superba*). Using a numerical model informed by 1 year of acoustic observations in the East Antarctic, we estimated the total particulate organic carbon (POC) flux from krill fecal pellets to be 9.68 milligrams of carbon per square meter per day (mg C m^{-2} day^{-1}). A maximum of 25% of krill migrated to depths >200 m with a strong seasonality component, transporting <10% of the total krill POC flux (1.28 mg C m^{-2} day^{-1}) to the deep ocean. Accurate carbon flux estimates are essential to inform climate policy and mitigation strategies, and models that include vertical migration will overestimate carbon export if this seasonality is not captured.

The biological carbon pump consists of a suite of processes that sequester carbon by vertical transfer to the deep ocean. Zooplankton are a major component of the biological carbon pump as they consume ~75% of daily phytoplankton production in the upper water column (*1*) and repackage the particulate organic carbon (POC) in phytoplankton into dense, fast-sinking fecal pellets. Yet fundamental questions exist around the mechanism and efficiency of this carbon transport to depth, which limits simulations of present and future climates, particularly for remote and productive regions like the Southern Ocean.

When released in the upper water column, zooplankton fecal pellets and other biogenic particles passively sink to depths where they are assumed to be sequestered for decades to millennia, a process known as the gravitational pump (*2*, *3*). However, sinking particles are vulnerable to attenuation (degradation) by fragmentation (coprohexy), reingestion (coprophagy), dissolution, and bacterial remineralization, all of which reduce the flux of POC to the deep ocean and limit the efficiency of the biological carbon pump (*4*, *5*).

Alongside gravitational sinking, there are physical and biological phenomena that inject carbon directly into deeper waters. Direct injection can increase the efficiency of the biological carbon pump as injected particles are less degraded than passively sinking particles (*3*, *5*). Physical processes include eddy subduction and seasonal vertical mixing of the water column, whereas biological mechanisms involve the migration of animals between the epipelagic (<200 m) and mesopelagic (>200 m) zones, a process known as the mesopelagic migrant pump (*3*). Carbon released through respiration, excretion, and egestion by migrating organisms can contribute up to 30% of total carbon flux in some regions (*6*). Using high-resolution field observations coupled with a numerical model (Fig. 1), we assess the contribution of a dominant Southern Ocean organism, *Euphausia superba* (Antarctic krill, hereafter krill), to seasonal POC export to the seafloor through gravity and migration.

Antarctic krill is a key micronekton species in Southern Ocean food webs with a circumpolar distribution and estimated biomass between 117 and 379 million tonnes (*7*), which constitutes the greatest biomass of a single wild animal species globally. Krill produce fast-sinking carbon-rich fecal pellets that export up to 40 million tonnes C $year^{-1}$ (*8*, *9*) and make up more than 90% of sediment trap material along the Antarctic coastline in summer (*10*). Krill, as well as other fish and zooplankton, perform diel vertical migration (DVM), typically feeding in the upper ocean (<50 m) at night and descending to depth (>100 m) during daylight hours (*11*, *12*). Seasonal vertical migrations also occur, in which organisms occupy the upper ocean in summer (50 to 100 m) and migrate to depth (100 to 200 m) during winter (*13*, *14*). Observations of krill since the 1980s (*15*, *16*) show that their behavior is not homogeneous across populations or environments. For example, deep-sea cameras have observed krill near the seafloor, mating at 750 m and feeding at 3500-m depth (*17*–*20*). Shipboard active acoustic surveys with net hauls have been the primary method of assessing krill populations and distributions, typically using echosounder data from the upper 250 m of the water column (owing to limitations imposed by sound attenuation). Full assessment of krill DVM is challenging using this technology and platform type, which is compounded in the Antarctic winter when sea ice prevents access by ships, and hence our understanding of seasonal krill ecology is incomplete.

Global models rely on observational insights to map the flow of carbon through marine systems. Despite awareness of the potential importance of krill and zooplankton to the biological carbon pump (*1*, *9*, *21*), little attention has been given to how the ecology of animals may influence biogeochemical processes (*22*–*24*). Presently, no climate models account for the effects of zooplankton vertical migration on the biological carbon pump (*22*). In this study, we collected data on krill migration using video footage and contemporaneous high-resolution echosounder data from a seafloor lander deployed at 387-m depth in Prydz Bay, East Antarctica (~200 km offshore), for 1 year (Fig. 2, A and B). The data were used to analyze how Antarctic krill vertical migration influences seasonal POC transfer to the deep ocean using a numerical model. The model (broadly described in Fig. 1) combined observations of nonmigrating and migrating krill densities with seasonal chlorophyll concentrations to estimate the amount of fecal carbon sinking from epipelagic to mesopelagic waters and the amount actively injected when migrating krill defecate at depth. We use the model to test assumptions about the magnitude of contributions from the gravitational pump and mesopelagic migrant pump to the total krill POC flux (*3*, *9*, *25*).

Seasonal patterns in krill numeric density and DVM

The echosounder provided high-resolution information (operating 7 min on, 7 min off, for 365 days) on krill density and behavior between the sea surface and seafloor, at a vertical resolution of 0.375 m (Fig. 2C; for krill-target-classified echograms, see fig. S1). Video footage revealed that acoustic targets above the mooring were predominantly krill (Fig. 2D). Integrated over the water column, the numeric density of all krill was on average 1350 individuals (ind) m^{-2} day^{-1} with a 95% confidence interval (CI) of 110–16,500 (Fig. 3A). Seasonal krill density was greatest in winter (2000 ind m^{-2} day^{-1}; 95% CI: 220–18,000), but reached a peak of 22,000 ind m^{-2} day^{-1} in September (Fig. 3A). This was followed by declines in spring (1400 ind m^{-2} day^{-1}; 95% CI: 80–23,500), summer (1500 ind m^{-2} day^{-1}; 95% CI: 160–11,500), and least density in autumn (500 ind m^{-2} day^{-1}; 95% CI: 50–5500). Density generally remained below 5000 ind m^{-2} day^{-1}

[1]Australian Antarctic Program Partnership, Institute for Marine and Antarctic Studies, University of Tasmania, nipaluna/Hobart, Tasmania, Australia. [2]Australian Antarctic Division, Kingston, Tasmania, Australia. [3]University of New Hampshire, Durham, NH, USA. [4]Aqualyd Limited, Wakefield, New Zealand. [5]Echoview Software Pty Ltd, Hobart, Tasmania, Australia.
*Corresponding author. Email: abigail.smith@utas.edu.au

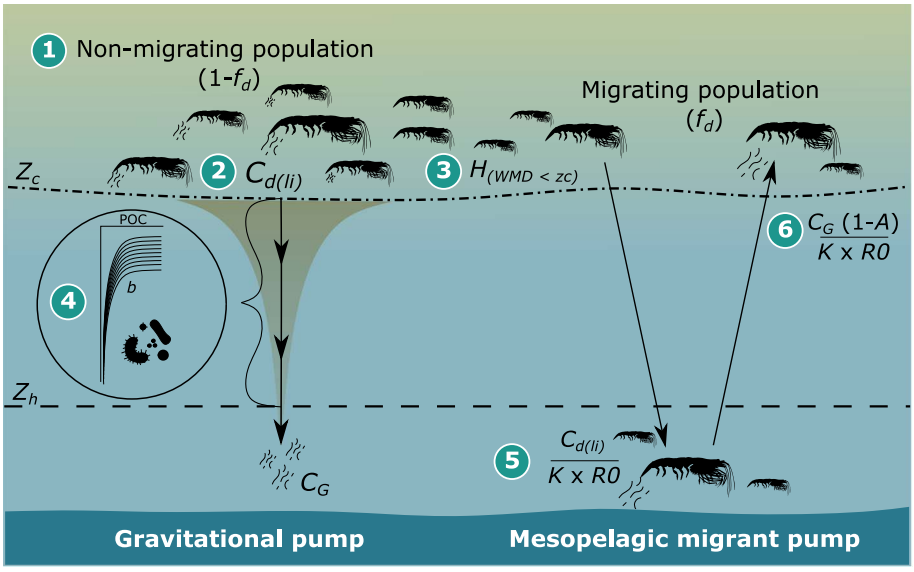

Fig. 1. Contribution of Antarctic krill fecal pellets to the gravitational pump and mesopelagic migrant pump estimated by a numerical model. (1) Nonmigrating (1-f_d) and migrating (f_d) krill populations. (2) Carbon egestion rates ($C_{d(li)}$) specific to krill length. (3) Daily carbon egestion on the basis of the number of hours per day (H) in which krill weighted mean depth (WMD) was shallower than the chlorophyll zone (z_c). (4) Fecal pellets released while krill occupied the z_c, sink to a carbon export depth (z_h) of 200 m and experienced losses defined by a power law with coefficient b; the carbon reaching depth via the gravitational pump (C_G) is therefore less than the POC originally egested by krill ($C_{d(li)}$). (5) Carbon exported by migrating krill was the same as nonmigrating krill but delivered one additional fecal pellet per individual below z_h, which experienced no attenuation; the concentration of POC in a single fecal pellet was defined as the fraction of carbon egested in the gut clearance rate period (K), which varies with seasonal respiration rates $R0$. (6) Carbon efflux by migrating krill calculated as in (5) but where ingested carbon is equivalent to depth-attenuated carbon C_G multiplied by the inverse of assimilation factor A. See materials and methods for the full model description.

between April to July and October to January, with some exceptions.

Krill DVM occurred year-round; however, the amplitude of these migrations varied seasonally (Fig. 2C). The weighted mean depth (*WMD*, i.e., the depth at which most krill were observed for a given hour) varied hourly and monthly because of diel and seasonal vertical migration, respectively. Migrators were defined as those krill moving between epipelagic (<200 m) and mesopelagic (>200 m) on a daily basis (*26*). If the daily *WMD* was <200 m, krill were classed as epipelagic migrators, and if daily *WMD* was >200 m, krill were classed as epibenthic migrators. Not all krill underwent vertical migration, and between 19 and 25% (95% CI) of the krill population (as a fraction of numeric density) participated in daily mesopelagic migrations. Most of these migrations occurred in winter when epibenthic krill communities most often spent time at depths below 200 m (Fig. 3B), but made daily excursions between epipelagic (<200 m) and mesopelagic (>200 m) waters. Over an annual cycle, 32% of krill migrated to a maximum depth of 371 m in winter as vertical migrations, whereas during summer, 5.4% of krill migrated to an average depth of 98 m in epipelagic migrations within the upper 200 m of the water column. Autumn and spring were transitional periods, in which 28% of krill migrated to 370 m in autumn and 19% migrated to the same maximum depth in spring. When averaged over the annual cycle, 22.4% of the total krill population migrated to a maximum depth of 372 m, with significant differences among seasons [$P = 3.42 \times 10^{-10}$, one-way analysis of variance (ANOVA) where seasons were independent groups] within krill DVM.

An upward-looking acoustic mooring deployed in the eastern Weddell Sea at 347-m depth for 10 months in 2005 (*27*) showed similar seasonality to Prydz Bay, albeit at a lower resolution (one ping per hour, integrated over 16-m vertical resolution). In February to May (late summer to autumn), 15% of the Weddell Sea mooring acoustic backscatter migrated from 150 to 200 m. This shifted to 53% between July and October (winter to spring) with migrations between 200 and 300 m (fig. S2). Overall, the fraction of migrators was greater in the Weddell Sea (95% CI: 35–39%) compared to Prydz Bay (95% CI: 19–25%), yet migrations occurred predominantly in winter months at both sites when chlorophyll concentrations are lowest (although the timing was offset by ~2 months). Such seasonality is also reflected in the literature (26 studies) across Antarctica, where shallow migrations (50 to 150 m) occur in summer and deeper migrations (80 to 210 m) occur in winter (fig. S3) (*13*, *15*, *28*–*34*). These patterns are observed across variable seafloor depths, both on the shelf (400-m depth) and off the continental shelf (5000-m depth).

Our seafloor echosounder showed that migrations to maximum depths commonly occurred between 05:00 and 17:00 local time (66.9°S, 75.0°E), despite variations in seasonal daylight hours (fig. S4). Throughout the year, krill spent on average 3.6 hours day^{-1} grazing in waters where chlorophyll concentrations [as detected by Biogeochemical-Argo floats (*35*, *36*)] were ≥0.05 mg chlorophyl *a* (chl-*a*) m^{-3} (dubbed the "chlorophyll zone", z_c), with more time (9.3 hours day^{-1}) in summer months compared to winter (2.6 hours day^{-1}, Fig. 3B). Krill were observed on camera near the seafloor in high numbers in autumn (Fig. 2D and movie S1). However, no useful footage was collected after 13 March 2021, owing to a defect with the camera system. Video footage showed krill fecal pellets released at depth; however, it is unclear whether these pellets are the result of feeding in the upper water column prior to migration or from feeding on mesopelagic food sources.

POC downward export by migrating and nonmigrating krill

Daily carbon egestion rates (C_d) defined by seasonal krill body length frequency distributions varied between 0.002 and 0.005 mg C ind^{-1} hour^{-1} over the year (figs. S5 and S6) (*37*). Combining seasonal egestion rates with daily numeric density of krill (ρ) and time spent grazing (H) in the z_c, and accounting for degradation of sinking fecal pellets, our one-dimensional model estimated the total carbon flux from all krill exported an annual average of 9.68 mg C m^{-2} day^{-1} (95% CI: 0.51–185; Fig. 4A). Of this, the nonmigrating population contributed 8.39 mg C m^{-2} day^{-1} (95% CI: 0.42–166) from sinking fecal pellets alone, whereas the migrating population contributed 1.28 mg C m^{-2} day^{-1} (95% CI: 0.04–45.3) from a combination of sinking fecal pellets plus vertical migration (Fig. 4A).

The large variability in the annual average POC flux is driven by the daily variability in krill density (95% CI: 110–16,500 ind m^{-2} day^{-1}; Fig. 5A); the occurrence of krill in the Southern Ocean is highly variable because of their tendency to form dense swarms. This is further compounded by seasonal changes in the migrating fraction of krill, number of hours spent in z_c, and krill metabolism. At this location on the continental shelf, total krill POC flux was greatest in summer (18.1 mg C m^{-2} day^{-1}; 95% CI: 1.3–260) followed by winter (11.7 mg C m^{-2} day^{-1}; 95% CI: 0.65–215) and spring (7.60 mg C m^{-2} day^{-1}; 95% CI: 0.60–97), with the lowest

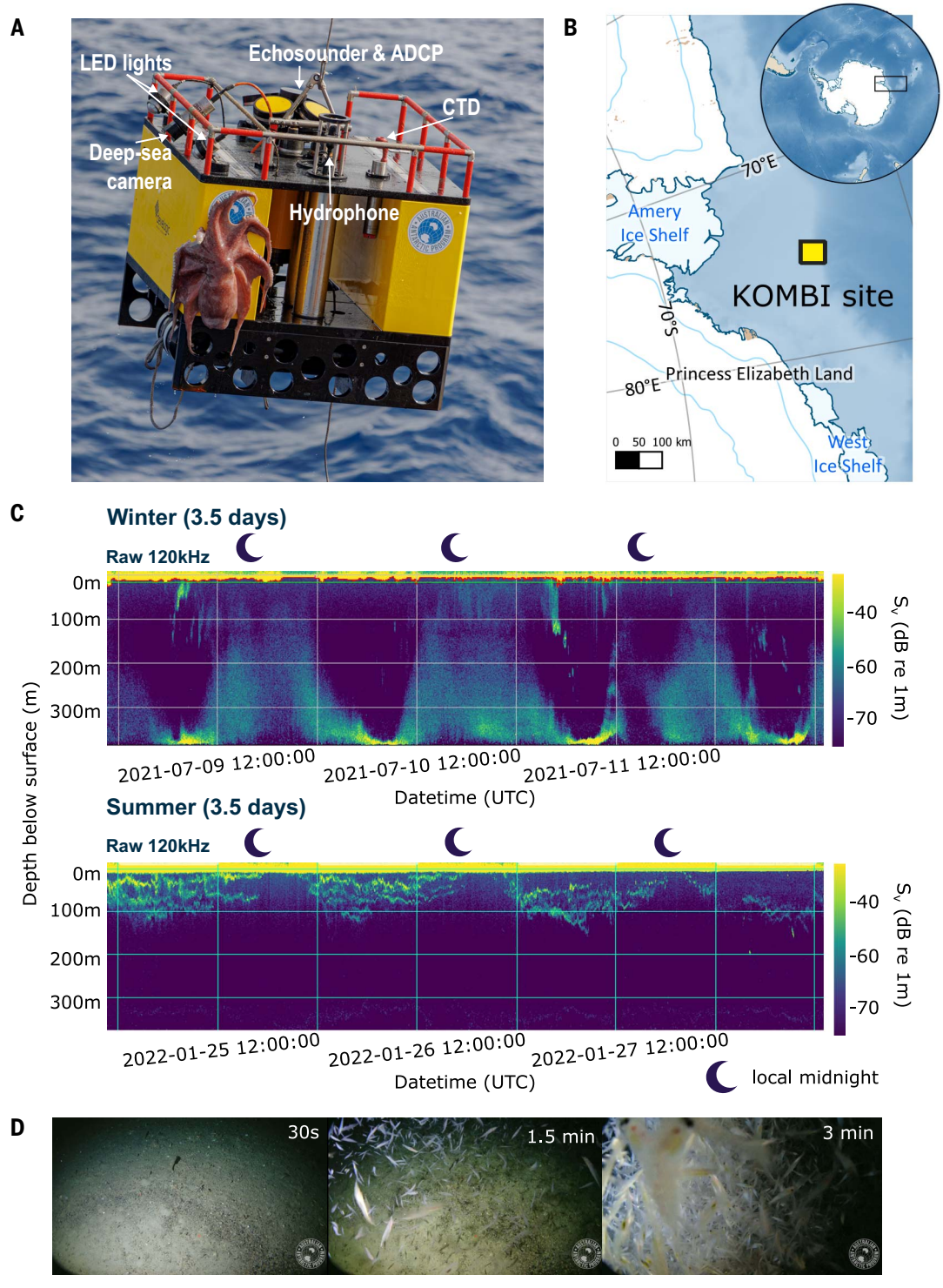

Fig. 2. Prydz Bay mooring deployment and data examples. (**A**) Krill Observational Mooring for Benthic Investigation (KOMBI)—a seafloor lander equipped with acoustic doppler current profiler (ADCP, 100 kHz), echosounder (70 and 120 kHz), deep-sea camera and lights, conductivity-temperature-depth (CTD) sensor, and passive acoustics hydrophone (not used in this study). This image also features an octopus carried to the surface by the lander upon retrieval. (**B**) Deployment location of KOMBI lander in Prydz Bay, East Antarctica. (**C**) Raw 120-kHz echograms recorded from the KOMBI for a representative 3.5 days of full water column DVM patterns in winter (top), and shallow migrations in summer (bottom). (**D**) Stills from video footage of krill near the seafloor (387 m) captured from the KOMBI, attracted by 2.5 min of illumination from the lights on the lander, used to ground truth echosounder target classification (movie S1).

POC flux in autumn (1.70 mg C m^{-2} day^{-1}; 95% CI: 0.05–48, Fig. 4A).

Sinking fecal pellets from the chlorophyll zone released by both the nonmigrating and migrating population experienced attenuation losses, which resulted in 23 to 60% of egested POC being retained in the epipelagic (<200 m, Fig. 4B). The amount of carbon deposited at depth by migrating krill represented on average 0.3% of the total annual carbon exported below 200 m. The greatest proportions of carbon deposited by DVM occurred in winter and late autumn but never contributed more than 6% to the total krill POC flux (Fig. 4B). Although the fraction of migrating krill increased in winter, this occurred when upper ocean POC concentrations were lowest and reduced krill metabolism limited carbon egestion.

POC upward efflux by migrating krill

Our observed ascent speeds combined with estimates of gut clearance rates from the literature (*38*, *39*) indicate that epibenthic migrating krill can transport benthic material to the upper water column before defecation occurs. Echograms show average ascent speeds of 104 m $hour^{-1}$, so traveling from a depth of 400 m to the upper 100 m of ocean would take 2.8 hours.

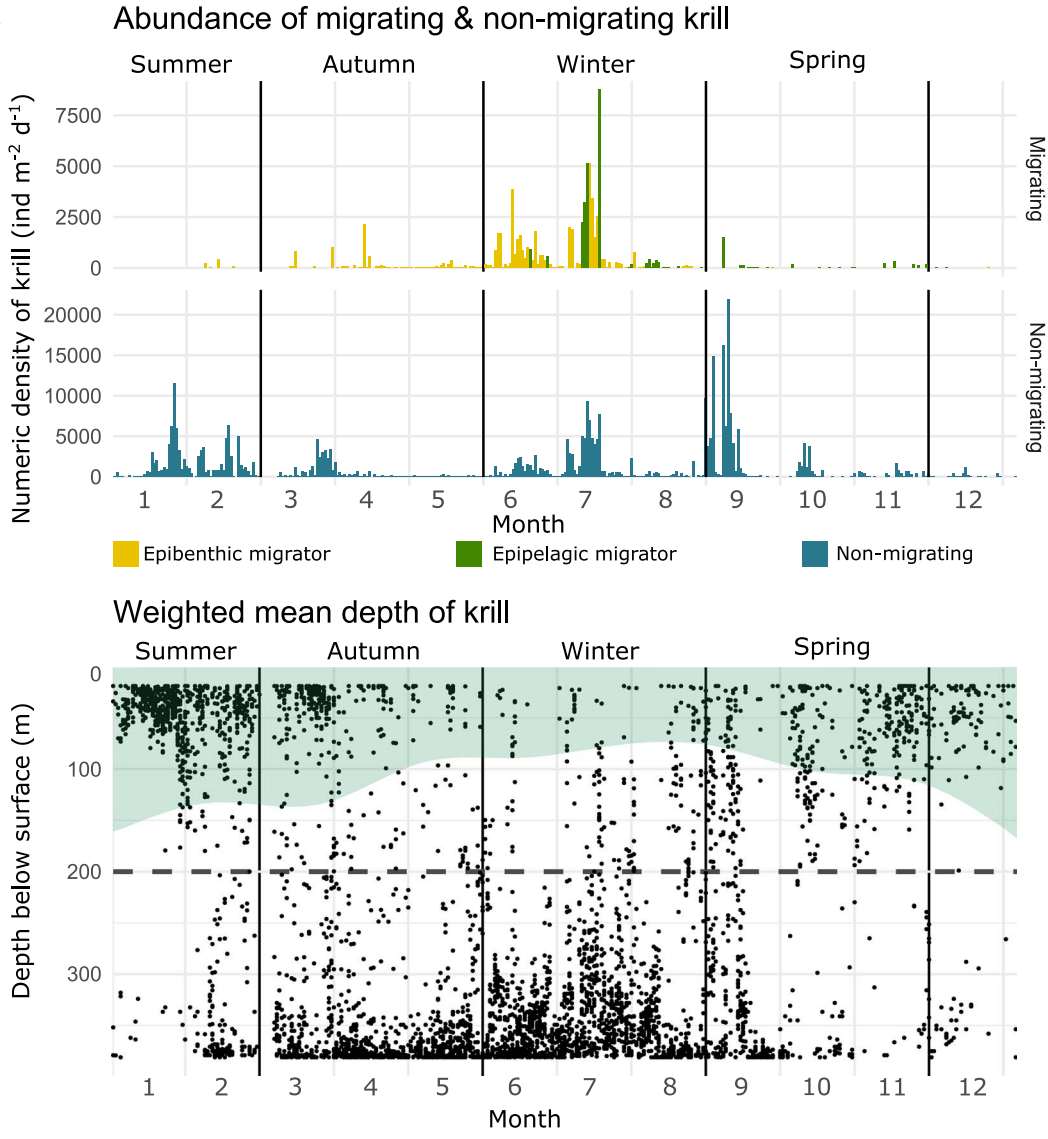

Fig. 3. Density and migration patterns for krill observed from the Prydz Bay mooring over 1 year. (**A**) Numeric krill density (ind m^{-2} day^{-1}) of migrating (top, epipelagic migrators in green, epibenthic migrators in yellow) and nonmigrating (bottom, blue) krill integrated over the water column throughout the year. Note the difference in scale for the *y* axis of migrating and nonmigrating krill density. (**B**) The weighted mean depth of krill calculated at hourly intervals reveals frequent excursions between the epipelagic (<200 m) and mesopelagic (>200 m) waters. Depths at which chlorophyll concentrations were >0.05 mg m^{-3} (as detected by Biogeochemical-Argo floats) are highlighted in green. Dashed line represents the interface between epipelagic and mesopelagic waters (200 m).

Given that mean gut turnover periods for krill average 7.9 hours (*38*), this suggests that krill would reach the upper water column before fully evacuating their gut contents, allowing them to transport benthic material to the epipelagic zone.

Epibenthic krill feeding on degraded organic particles (such as marine snow, detritus, or other fecal pellets) have the capacity to reintroduce 35% of the material previously injected to depth back into epipelagic waters. This represents a return of 2.2% of the total krill POC flux. This estimate assumes that krill ingest degraded carbon at depth (i.e., carbon ingestion is lower at depth, because carbon availability at depth is lower). However, studies have shown that krill may vary their feeding rates to achieve a consistent egestion rate (*38*, *40*, *41*), in which case POC export will equal resuspension, resulting in a near net zero transport of POC. Consumption of organic material in sediments may increase carbon egestion rates of epibenthic krill; however, there are little supporting data to date for carbon egestion rates of krill with benthic or detrital diets.

Discussion

We assessed the POC flux from Antarctic krill by means of sinking fecal pellets and vertical migration using 1 year of acoustic observations. Mean POC flux from fecal pellets was 9.68 mg C m^{-2} day^{-1} (95% CI: 0.5–185), peaking in summer and winter. Fecal pellets sinking from epipelagic waters contributed most to total krill POC flux, whereas migrating krill injected only 0.25 to 0.44% (95% CI; maximum 6.3%) into mesopelagic waters, suggesting that the krill mesopelagic migrant pump is up to a factor of 40 smaller than previous estimates (*42*, *43*).

The krill mesopelagic migrant pump was most efficient at transporting carbon in winter when krill migration spanned the full water column. In summer, migrations into the mesopelagic zone (200 m) rarely occurred, leading to degradation of sinking fecal pellets from their release depth in the upper ocean. Similar patterns of seasonal variation in migration are evident from extensive sampling throughout the Southern Ocean (fig. S3) (*13*, *15*, *28*–*34*), including moored instruments in the eastern Weddell Sea (fig. S2) (*27*, *29*).

Our carbon flux estimates represent an upper limit of the POC transported by migrating krill as we assumed no defecation during migrations, so that each individual transported one full gut of POC each to mesopelagic waters. Krill have been observed to sink when sated (*42*), and individuals may release fecal pellets during their descent, allowing for further attenuation of POC from particles released higher in the water column. With these factors, it is likely that active transport of POC by migrating krill is even lower than the values presented here.

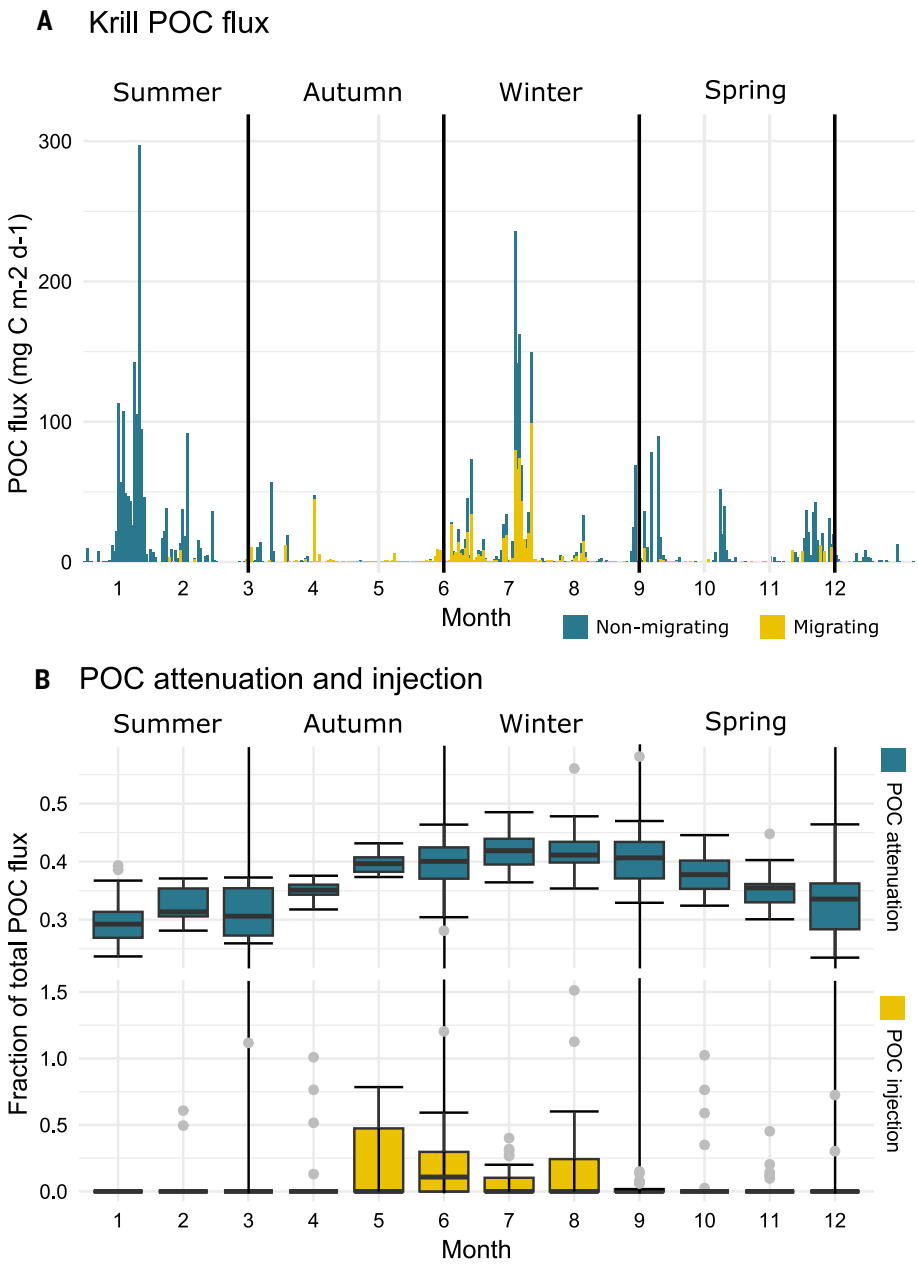

Fig. 4. Particulate organic carbon flux from nonmigrating and migrating krill over 1 year. (**A**) Total POC flux released by migrating and nonmigrating krill that reaches mesopelagic waters via nonmigrating (blue) and migrating (yellow) krill. (**B**) Fraction of the total POC released by the krill population that is attenuated as particles sink (blue) compared to the fraction of total POC that is injected into the mesopelagic by DVM (yellow). Each boxplot is composed of the following fraction of total POC flux summary statistics: median, solid black center; lower and upper quartiles, lower and upper box edges; and 1.5× the interquartile range solid black upper and upper bars (whiskers) and points outside the bars, solid gray points.

The fraction of krill migrating into the mesopelagic varied seasonally and rarely reached 50% in our Prydz Bay study and the separate study conducted by Cisewski *et al.* (*27*, *29*) in the Weddell Sea. In the absence of observational data, previous studies have used simplified DVM patterns (12-hour cycle, 50% population migrating below 200 m) to represent DVM in the mesopelagic migrant pump (*44*), which could inadvertently introduce large biases. Assuming a consistent 50% migrating population year-round in our model resulted in a 216% overestimation of carbon injection by krill, when compared with direct observations of migrating populations.

The broad uncertainty in annual POC flux is due to high daily variability in krill density (Fig. 5A). Total POC flux estimates align with the lower end of previously reported sediment trap fluxes around the Antarctic Peninsula (8.5 to 50.2 mg C m^{-2} day^{-1}) (*37*) and South Georgia, where krill fecal pellets make up 52% of the matter (2.5 to 463 mg C m^{-2} day^{-1}) (*8*). Higher krill densities in the Atlantic sector (30 g m^{-2}) (*45*) compared to East Antarctica (8.3 g m^{-2}) (*32*) may explain the elevated POC flux measured in the west. Our shelf-based echosounder data revealed an increase in krill densities throughout winter, consistent with the southward migration of winter krill (*46*). Lateral migrations between pelagic and shelf environments highlight the need for increased spatial coverage to assess seasonal krill carbon fluxes across the Southern Ocean.

Previous studies have suggested that krill have the capacity to undertake multiple vertical migrations within a 24-hour period (*42*), potentially increasing POC injection to depth. We found that krill typically migrated once per day and that POC injection was most sensitive to grazing parameters (number of hours spent in the chlorophyll layer and gut clearance rate) and attenuation processes (Fig. 5B). This reinforces the importance of observing and modeling vertical migration in future studies. Indeed, grazing has already been identified as a source of uncertainty in Earth system models (*23*), and the contribution of vertical migration to POC export may shift as future climate conditions alter krill metabolism, behavior, food availability, and associated microbial productivity.

This model focused on the POC flux from fecal pellets; however, the molting of exoskeletons (*8*), excretion (*47*), respiration (*9*), and use of lipid reserves (*48*) also contribute to dissolved and particulate carbon fluxes by krill over seasonal and diel scales, so they should also be captured in future modeling work. Our calculations suggest that migrating epibenthic krill also have the capacity to resuspend 35% of previously exported material from the seafloor to epipelagic waters during their ascent. However, efflux estimates here are likely underestimated because krill have been observed to consume organic material from the seafloor (*40*), which if brought to the upper water column may further reduce the efficiency of the biological carbon pump.

Antarctic krill play an important role in the biological carbon pump, but without observational data, we risk using inaccurate and misleading assumptions about behaviors that influence carbon export and climate models. By modeling with 1 year of high-resolution observations of krill density and behavior, we have clearly shown that sinking fecal pellets dominate krill carbon export, with only a minor contribution from vertical migrations, which vary on a seasonal basis.

Constraining other components of POC flux (grazing, particle attenuation, remineralization, and respiration) with observational data remains a high priority to improve circumpolar

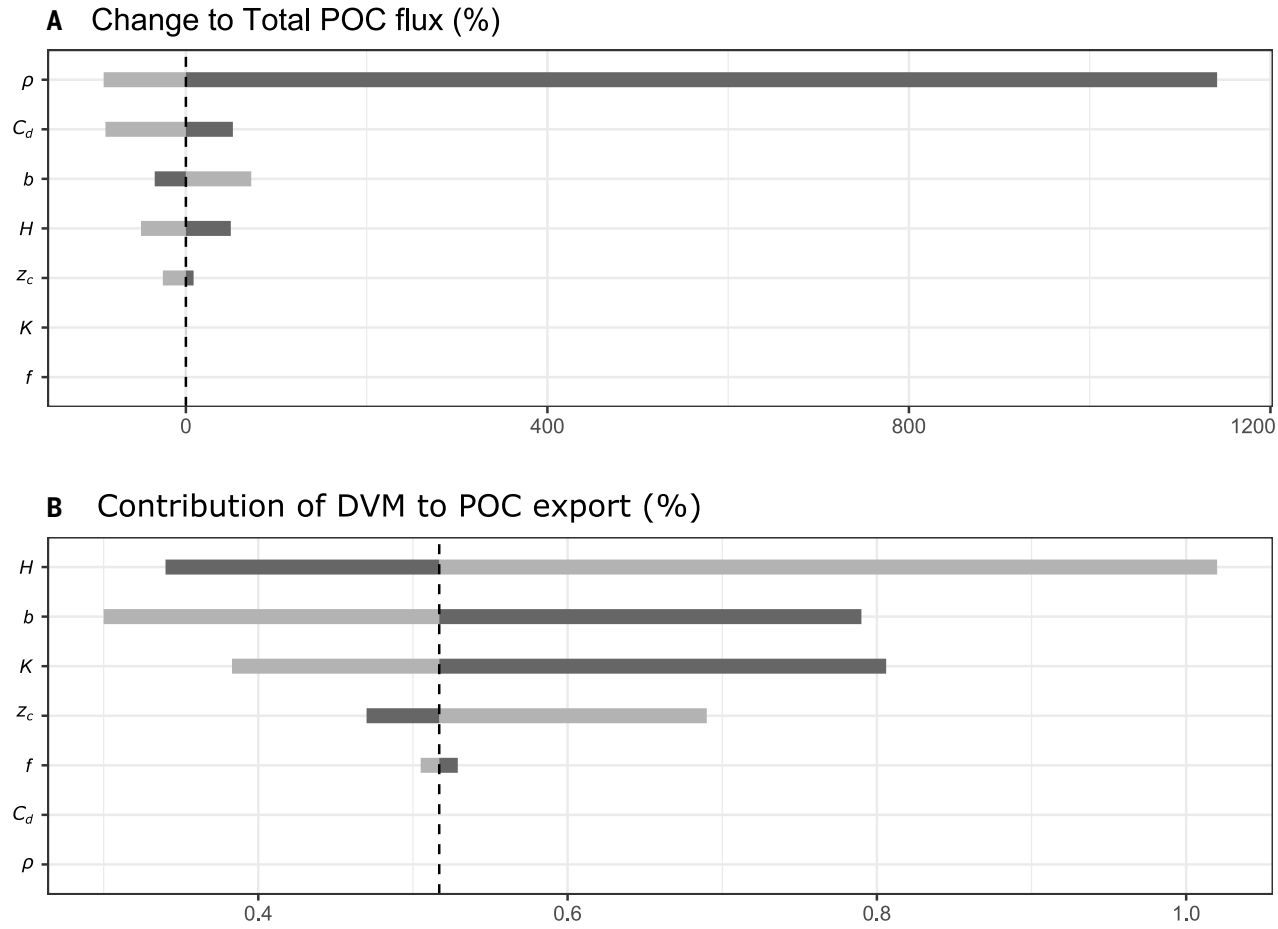

Fig. 5. Sensitivity of the biogeochemical model to parameter perturbations. Twenty-fifth (light gray) and 75th (dark gray) percentile influencing (**A**) the change in total POC flux and (**B**) the overall contribution of DVM to POC export (as the percentage of total material at the seafloor delivered by migrating krill. ρ, numeric density; *b*, attenuation curve exponent; *H*, grazing hours; *f*, migrating fraction; C_d, egestion rate; z_c, surface phytoplankton layer depth; *K*, gut clearance rate.

estimates of carbon export by krill in the Southern Ocean. We strongly recommend incorporating seasonal variability into biogeochemical models that account for krill DVM to prevent overestimating POC export by the mesopelagic migrant pump. Improving our understanding of interactions between zooplankton ecology and biogeochemical cycles is crucial to accurately simulating carbon flux under present and future climate scenarios.

Materials and methods

Krill Observational Mooring for Benthic Investigation (KOMBI)

Observational data were collected from a purpose-built seafloor lander, which was deployed at 387-m depth, near the shelf break in Prydz Bay, East Antarctica (66.95°S, 75.01° E; Fig. 2B). The lander collected data between 6 March 2021 and 14 March 2022.

The lander was equipped with four scientific instruments (Fig. 2A): an RBR*concerto*^{3} conductivity-temperature-depth (CTD) logger (measuring at 10-min intervals), a develogic MP.CAM 4K camera with two develogic UW. L75 LED lights (recording 2.5 min of illuminated footage at 5-hour intervals), a hydrophone (not used in this study), and a Nortek Signature100 comprising a 100-kHz acoustic Doppler current profiler (ADCP) and scientific echosounder (operating at 70 and 120 kHz in continuous-wave, narrowband mode) mounted on a gimbal to ensure vertical orientation.

The Nortek Signature100 was deployed using the settings in Table 1. The echosounder was calibrated in a 10,000-liter tank filled with seawater chilled to 0.1°C with a 23-mm-diameter tungsten carbide sphere. Calibration S_v offsets (Table 1) for both frequencies were applied in postprocessing.

Active acoustic data processing

Echosounder data were processed using Echoview version 13.0.398 (Echoview Software Pty Ltd, Hobart, Australia). Narrowband data from both the 70- and 120-kHz channels were cleaned using Echoview's attenuated signal removal, impulse noise removal, and background noise removal operators (*49*, *50*). Signal beyond the air-water interface or air–sea ice interface was detected and removed using threshold offset lines on a 7 × 7 convolution of the 70-kHz data between 0- and 250-m depth (to exclude keels of deep icebergs).

Target classification using dB differencing (120 − 70 kHz) was performed to discern krill echoes in the acoustic data. To capture target strength variability with vertically migrating krill [as a result of variable orientation (*51*)], a dB-differencing envelope of −4.4 to +5.7 dB was used, encompassing the target strength of krill from 14- to 60-mm length at a random uniform distribution of tilt angles. Target-classified 120-kHz S_v data were thresholded at −70 dB re 1 m^{-1}, and background noise [estimated from (*50*)] in the upper water column (range 372 m from instrument) was on average −66.5 dB re 1 m^{-1}, therefore krill densities lower than 7.5 ind m^{-3} between 15 and 61 m depth may be underestimated (fig. S7). Krill 120-kHz data were integrated as 1-m depth by 1-hour integrated cells between 15 and 385 m.

Table 1. Parameters used by the Nortek Signature 100. For the ADCP, pings were transmitted and received at the noted ping interval and then averaged to yield one measurement per averaging interval. Within each ping interval, all three pulse types occurred sequentially. CW, continuous wave; n/a, not applicable.

Parameter	Echo 70 kHz CW	Echo 120 kHz CW	ADCP 100 kHz
Operation periods (time on/time off) (s)	420/420	420/420	420/420
Ping interval (s)	6	6	6
Averaging interval (s)	n/a	n/a	420
Profile range (m)	2–400	2–400	2–299
Range resolution (m)	0.375	0.375	3
Pulse duration (ms)	1	1	n/a
Calibration offset (S_v, dB re 1 m^2/m^3)	−43.1	−47.2	n/a
Equivalent beam angle (sr)	0.0300*	0.0105*	n/a
3 dB two-way beamwidth (°)	13.2*	7.8*	n/a

*Default factory settings.

Numeric density of migrating and nonmigrating krill

Converting acoustic backscatter to numeric or biomass density requires length frequency distributions for the population; however, these data are sparse for krill in winter months (April to November), particularly for remote East Antarctic regions. To estimate monthly length frequency distributions, we used data from net hauls collected in East Antarctica between 1977 and 2021 (fig. S6), combined with krill lengths in the Southern Ocean Diet and Energetics Database (*52*). Where data were sparse, we interpolated frequency data across 1-mm-length bins using a Generalized Additive Model (see supplementary text section 4).

Numeric density (ρ) was calculated from the mean area backscattering coefficient, s_a (*53*), integrated over all depth bins for a 1-hour interval. If p_{im} is the proportion of krill in ith length class in month m, then the expected total s_a generated by N krill is

$$s_a = N \sum_i p_{im} \sigma_i \quad (1)$$

where the backscattered acoustic power from a single krill of the ith length class is given by the linear form of target strength σ_i (*54*). Therefore, the numeric density of krill can be estimated by

$$N = \frac{s_a}{\sum_k p_{km} \sigma_k} \quad (2)$$

Migrating krill are defined as those moving between epipelagic (<200 m) and mesopelagic (>200 m) waters. Klevjer *et al.* (*26*) calculated the migrating zooplankton fraction using the ratio of mesopelagic s_a between day and night. Because our data showed krill migration between 05:00 and 17:00 local time (fig. S4), we defined the migrating fraction f_d as follows:

$$f_d = 1 - \frac{s_{a(N_{zh})} DNR}{s_{a(D_{zh})}} \quad (3)$$

where $s_{a(Nzh)}$ is the mean s_a below depth z_h between 17:00 and 05:00, and inversely, $s_{a(Dzh)}$ is the mean s_a below z_h between 05:00 and 17:00. The mesopelagic zone z_h was defined as deeper than 200 m (*26*, *44*), and a day-to-night ratio *DNR* was used to standardize the daily backscatter across the whole water column,

$$DNR = \frac{s_{aN}}{s_{aD}} \quad (4)$$

with $s_{a(N)}$ and $s_{a(D)}$ representing the total backscatter across the whole water column for the "night" and "day" hours, respectively.

The daily numeric density of migrating krill (ρ_m) in ith length class is the fraction f_d of mean daily s_a for the water column multiplied by the backscattering cross section for that population

$$\rho_m = s_a \sum_i \left[\frac{p_i(f_d)}{\sum_k p_k \sigma_k} \right] \quad (5)$$

where p_i is the proportion of individuals in length class i for a given month and σ_i is the backscattering cross section of an individual in that length class. Conversely the numeric density of nonmigrating krill (ρ_{nm}) is

$$\rho_{nm} = s_a \sum_i \left[\frac{p_i(1 - f_d)}{\sum_k p_k \sigma_k} \right] \quad (6)$$

determined by taking the inverse fraction of migrating krill ($1 - f_d$).

A weighted mean depth *WMD* (*26*, *55*, *56*) was used to identify DVM patterns from acoustic backscatter and was defined as

$$WMD = \frac{\sum s_{aj} D_j}{\sum_j s_a} \quad (7)$$

where the sum of s_a in depth stratum j was multiplied by the depth D_j, and divided by the total sum of backscatter integrated over that hour.

Mechanistic model to quantify krill-driven POC export

To estimate daily POC flux from krill, we combined numeric density, migrating fraction, and *WMD* from echosounder data with literature estimates of daily carbon egestion and POC attenuation. Carbon egestion was defined by monthly krill length distributions and limited to hours when krill were in the "chlorophyll zone" (depths shallower than z_c with sufficient chlorophyll a for feeding). All model parameters are listed in Table 2, with a conceptual overview in Fig. 1.

The z_c included waters from 0 m to the maximum depth at which chlorophyll concentrations were sufficient for krill feeding [0.05 mg chl a m^3 (*57*)]. As chlorophyll fluorescence decreases with depth, krill were assumed to feed and egest continuously while present at depths shallower than z_c. Daily z_c ranged from 90 to 200 m over the 365 days (fig. S8) and was sourced from Biogeochemical-Argo (BGC-Argo) float profiles located between 60°–70°S, 55°–85°E, collected between 2016 and 2023 (*35*, *36*, *58*).

Daily carbon egestion C_d for krill of length i was described using a power law for hourly carbon egestion from body length,

$$C_{di} = 2 \times 10^{-8} l_i^{3.2859} \times H \quad (8)$$

parameterized from Pauli *et al.* (*37*) (fig. S5). Here, H is the sum of hours per day in which *WMD* is shallower than z_c, and because constant gut clearance rates have been observed under variable food concentrations (*40*, *59*, *60*), we assume that krill feed and egest continuously for the duration of H.

Martin's curve was used to quantify POC attenuation (*61*). Martin's curve estimates the carbon C_h reaching depth z_h from the carbon C_0 released at the time of egestion from depth z_0 through

$$C_h = C_0 \left(\frac{z_h}{z_0} \right)^{-b} \quad (9)$$

where the flux attenuation coefficient b is −0.3 for polar waters (*43*, *61*, *62*) (supplementary text section 6).

Table 2. Symbols, units, and definitions for parameters used in the mechanistic POC flux model. KOMBI: Krill Observational Mooring for Benthic Investigations; Var, variable.

Symbol	Unit	Definition	Value	Source
s_a	1	Acoustic backscatter for krill integrated over water column	Var	KOMBI
p_i	–	Proportion of individuals in length class *i*	Var	Net hauls and predator gut contents (*52*)
f_d	–	Fraction of migrating krill	Var	KOMBI
σ_i	m^2	Backscattering cross-section of length class *i*		(*67*)
WMD	m	Weighted mean depth	Var	KOMBI
z_c	m	Maximum depth of the chlorophyll layer where krill feed	Var	(*35*, *58*)
z_h	m	Mesopelagic export depth	200	(*26*, *44*)
b	-	Martin's curve attenuation coefficient	−0.3	(*43*)
C_{di}	mg C ind^{-1} day^{-1}	Daily carbon egestion for krill of length class *i*	Equation 8	(*37*)
l_i	mm	Krill body length class	Var	Net hauls and predator gut contents (*52*)
H	h	Hours where krill *WMD* was shallower than the maximum depth of the z_c	Var	KOMBI
K	h^{-1}	Gut clearance rate	0.126	(*38*)
R0	-	Respiration factor	Var	(*64*)

By assuming krill egest continuously within the z_c, fecal pellets could be released anywhere between 15 m and z_c. We therefore rearranged Eq. 9 so that the average carbon C_h reaching z_h was

$$\overline{C}_h = \frac{1}{z_c}\int_{15}^{z_c} C_0\left(\frac{z_h}{z_0}\right)^{-b} dz_0 = \frac{C_0}{1+b}\left(\frac{z_h}{z_c}\right)^{-b} \quad (10)$$

representing the average carbon attenuation implied by the Martin's curve for a pellet released at any depth within the z_c. A depth of 200 m was used to define the upper boundary of the mesopelagic layer z_h into which carbon is considered exported (*44*, *63*) [but see (*5*, *43*) and supplementary text section 6].

The daily POC flux from nonmigrating krill (POC_{nm}) in each length class is calculated by multiplying the numeric density (Eq. 6), carbon egested in the z_c (Eq. 8), and attenuation during particle sinking (Eq. 10). The total POC flux is the sum of all length class contributions

$$POC_{nm} = s_a \sum_i \left[\frac{p_i(1-f_d)}{\sum_k p_k\sigma_k}\right]\left[C_{di}(1+b)^{-1}\left(\frac{z_h}{z_c}\right)^{-b}\right] \quad (11)$$

Likewise, for the hours in which migrating krill occupy the z_c, their POC flux will be driven by Eq. 11. However, we assume that each individual leaves the z_c with a full gut and does not defecate during migration, thereby transporting one additional gut full of POC per individual to the mesopelagic. Therefore, the expected total POC flux from migrating krill (POC_m) is

$$POC_m = s_a \sum_i \left[\frac{p_i(f_d)}{\sum_k p_k\sigma_k}\right]\left[C_{di}(1+b)^{-1}\left(\frac{z_h}{z_c}\right)^{-b} + \frac{C_{di}}{K \times R0}\right] \quad (12)$$

where gut clearance rate *K* is used to specify the mass of carbon released in a single pellet from the carbon egestion rate. Gut clearance rates were seasonally mediated with a respiration factor *R0* (*64*), which linearly reduced *K* over 45 days to 50% in winter and increased to 100% in summer.

Epibenthic migrating krill may contribute to carbon efflux by reintroducing POC from depth to surface waters. Although krill have been observed feeding on detritus at depth, data on carbon egestion rates from sediment-derived organic material is limited. Therefore, we estimated krill POC efflux by assuming that (i) krill feed on sinking material between 200 and 387 m but not on sediments; (ii) carbon ingestion follows the Martin curve (*61*); (iii) krill assimilate 42% of ingested carbon, egesting 58% (*40*); and (iv) epibenthic migrators transport one gut-full of carbon to the surface. Carbon efflux (POC_{eff}) was then calculated as

$$POC_{eff} = \left[\frac{C_G(1-A)}{K \times R0}\right] \quad (13)$$

where z_m is the maximum depth of the water column (387 m), *A* is the proportion of ingested carbon that is assimilated, and C_G is the carbon remaining after attenuation,

$$C_G = \frac{C_{di}\ z_m\left(z_m^{(1-b)} - z_h^{(1-b)}\right)}{(1-b^2)(z_m - z_h)} \quad (14)$$

which is integrated across z_m and the mesopelagic depth z_h.

Sensitivity analysis

A local sensitivity analysis was used to assess parameters with the most influence on total POC flux, and the contribution of DVM to exported POC at depth. Each factor in the model was individually changed by the 25th and 75th percentile of its observed variability, either from this study or literature values. Changes in total POC flux and DVM importance were compared to a base run, where ρ = 1350 ind^{-1} m^{-2}, f = 0.5, C_d = 0.03 mg C ind^{-1} $hour^{-1}$, H = 12 hours, K = 0.144 $hour^{-1}$, b = 0.32, and z_c = 150 m. Variability in numeric density (ρ) was taken from observations collected from the mooring, whereas variability in the chlorophyll zone (z_c) was taken from Biogeochemical-Argo float data. The number of hours spent grazing in the surface phytoplankton layer was taken as 6 and 18 hours out of a 24-hour period. Variability in the migrating fraction of krill was taken from f values calculated from the Prydz Bay KOMBI echosounder data, as well as a Weddell Sea moored ADCP backscatter (*27*). Sensitivity analyses were also performed using the summer and winter mean of f from both moorings owing to the significant seasonality in the data. Sensitivity to

POC egestion rates (*39*, *40*, *65*, *66*), gut clearance rates (*38*, *40*, *66*), and Martin's *b* (*62*) was assessed from values available in the literature.

Total krill POC flux was most sensitive to the numeric density of krill ρ, carbon egestion rate (C_d), the exponent of the particle attenuation curve (Martin's *b*), and the number of hours spent grazing (*H*, Fig. 5A). The percentage of POC at depth that was delivered by migrating krill can be used to assess the relative contribution of DVM to POC export (Fig. 5B). Alterations to *H*, *b*, and *K* had the largest influence on the contribution of DVM to POC export.

Varying ρ (25th to 75th percentile: 110 to 16,700 ind m^{-2}) changed the total flux of POC to the seafloor by several orders of magnitude (24.5 to 3750 mg C m^{-2} day^{-1}); however, increasing this parameter had no effect on the contribution of DVM to export because although the magnitude of individuals increases, the percentage of contribution does not change. Variability in the migrating fraction *f* was small across the combined acoustic backscatter from moorings in Prydz Bay and the Weddell Sea (25th to 75th percentile = 29.1 to 30.5%) and resulted in minor fluctuations to the contribution of DVM (0.01% change). Reducing *f* to summer values of 17% caused a 42% reduction in POC injection by DVM; however, this had little effect on the overall total POC flux (0.2% decrease) as nonmigrating krill delivered the majority of POC to depth via the gravitational pump.

Modifying carbon egestion rate C_d on the basis of literature observations (*38*–*40*, *65*, *66*) (25th to 75th percentile: 0.003 to 0.041) resulted in a −89% decrease to 52% increase in the total carbon flux. However, like ρ, changes to C_d influenced the magnitude of total POC flux but did not influence the proportion of total POC injected at depth with migrations.

By contrast, adjusting the exponent of the particle attenuation curve *b* by −0.13 to 0.78 [the 25th and 75th percentile of values reported in the literature (*43*, *62*) and references therein)] resulted in a 72% and −35% change to the total POC flux, respectively. Increasing attenuation reduces the amount of POC reaching the seafloor via sinking fecal pellets and thereby increases the contribution from DVM in delivering POC to depth.

Altering grazing hours *H* from 12 to 18 hours had the largest influence on the contribution of DVM to export. In this scenario, a greater number of fecal pellets are produced in the z_c, consequently increasing total POC export overall but reducing the fraction of POC delivered via DVM. Similarly, changes to the z_c influence grazing and the extent of particle attenuation with depth. Changes to gut clearance rate *K* from the literature (*38*–*40*) (25th to 75th percentile: 0.11 to 0.23 $hour^{-1}$) altered the amount of POC released in a single fecal pellet as a fraction of C_d. For example, a migrating krill with a carbon egestion rate of 0.004 mg C ind^{-1} $hour^{-1}$ and gut clearance rate of 0.126 $hour^{-1}$ would release 0.504 μg C in a single pellet and increasing *K* by 10% to 0.138 $hour^{-1}$ means a higher proportion of carbon is egested in a single pellet, raising egestion to 0.554 μg C per pellet. Full results from the sensitivity analysis are provided in supplementary text section 7 (table S1).

REFERENCES AND NOTES

1. D. K. Steinberg, M. R. Landry, Zooplankton and the Ocean Carbon Cycle. *Annu. Rev. Mar. Sci.* **9**, 413–444 (2017). doi: 10.1146/annurev-marine-010814-015924; pmid: 27814033
2. D. A. Siegel, T. DeVries, I. Cetinić, K. M. Bisson, Quantifying the Ocean's Biological Pump and Its Carbon Cycle Impacts on Global Scales. *Annu. Rev. Mar. Sci.* **15**, 329–356 (2023). doi: 10.1146/annurev-marine-040722-115226; pmid: 36070554
3. P. W. Boyd, H. Claustre, M. Levy, D. A. Siegel, T. Weber, Multi-faceted particle pumps drive carbon sequestration in the ocean. *Nature* **568**, 327–335 (2019). doi: 10.1038/s41586-019-1098-2; pmid: 30996317
4. M. H. Iversen, L. K. Poulsen, Coprorhexy, coprophagy, and coprochaly in the copepods *Calanus helgolandicus*, *Pseudocalanus elongatus*, and *Oithona similis*. *Mar. Ecol. Prog. Ser.* **350**, 79–89 (2007). doi: 10.3354/meps07095
5. K. O. Buesseler, P. W. Boyd, E. E. Black, D. A. Siegel, Metrics that matter for assessing the ocean biological carbon pump. *Proc. Natl. Acad. Sci. U.S.A.* **117**, 9679–9687 (2020). doi: 10.1073/pnas.1918114117; pmid: 32253312
6. M. H. Conte, "Oceanic Particle Flux" in *Encyclopedia of Ocean Sciences*, J. K. Cochran, H. J. Bokuniewicz, P. L. Yager, Eds. (Academic Press, ed. 3, 2019), pp. 192–200; https://doi.org/10.1016/B978-0-12-409548-9.11481-2.
7. S. Kawaguchi *et al*., Climate change impacts on Antarctic krill behaviour and population dynamics. *Nat. Rev. Earth Environ.* **5**, 43–58 (2024). doi: 10.1038/s43017-023-00504-y
8. C. Manno *et al*., Continuous moulting by Antarctic krill drives major pulses of carbon export in the north Scotia Sea, Southern Ocean. *Nat. Commun.* **11**, 6051 (2020). doi: 10.1038/s41467-020-19956-7; pmid: 33247126
9. E. L. Cavan *et al*., The importance of Antarctic krill in biogeochemical cycles. *Nat. Commun.* **10**, 4742 (2019). doi: 10.1038/s41467-019-12668-7; pmid: 31628346
10. M. R. Gleiber, D. K. Steinberg, H. W. Ducklow, Time series of vertical flux of zooplankton fecal pellets on the continental shelf of the western Antarctic Peninsula. *Mar. Ecol. Prog. Ser.* **471**, 23–36 (2012). doi: 10.3354/meps10021
11. A. S. Brierley, Diel vertical migration. *Curr. Biol.* **24**, R1074–R1076 (2014). doi: 10.1016/j.cub.2014.08.054; pmid: 25458213
12. R. M. Ross, L. B. Quetin, C. M. Lascara, "Distribution of Antarctic Krill and Dominant Zooplankton West of the Antarctic Peninsula" in *Foundations for Ecological Research West of the Antarctic Peninsula*, R. M. Ross, E.E. Hofmann, L. B. Quetin, Eds., Antarctic Research Series (1996), pp. 199–217. doi: 10.1029/AR070p0199
13. C. M. Lascara, E. E. Hofmann, R. M. Ross, L. B. Quetin, Seasonal variability in the distribution of Antarctic krill, *Euphausia superba*, west of the Antarctic Peninsula. *Deep Sea Res. Part I Oceanogr. Res. Pap.* **46**, 951–984 (1999). doi: 10.1016/S0967-0637(98)00099-5
14. D. Bahlburg *et al*., Plasticity and seasonality of the vertical migration behaviour of Antarctic krill using acoustic data from fishing vessels. *R. Soc. Open Sci.* **10**, 230520 (2023). doi: 10.1098/rsos.230520; pmid: 37771962
15. M. Godlewska, Z. Klusek, Vertical distribution and diurnal migrations of krill—*Euphausia superba* Dana—from hydroacoustical observations, SIBEX, December 1983/January 1984. *Polar Biol.* **8**, 17–22 (1987). doi: 10.1007/BF00297159
16. Y. Simmard, G. Lacroix, L. Legendre, Diel vertical migrations and nocturnal feeding of a dense coastal krill scattering layer (*Thysanoessa raschi* and *Meganyctiphanes norvegica*) in stratified surface waters. *Mar. Biol.* **91**, 93–105 (1986). doi: 10.1007/BF00397575
17. S. Kawaguchi, R. Kilpatrick, L. Roberts, R. A. King, S. Nicol, Ocean-bottom krill sex. *J. Plankton Res.* **33**, 1134–1138 (2011). doi: 10.1093/plankt/fbr006; pmid: 21655471
18. M. K. Kane, A. Atkinson, S. Menden-Deuer, Lowered cameras reveal hidden behaviors of Antarctic krill. *Curr. Biol.* **31**, R237–R238 (2021). doi: 10.1016/j.cub.2021.01.091; pmid: 33689718
19. A. Clarke, P. A. Tyler, Adult antarctic krill feeding at abyssal depths. *Curr. Biol.* **18**, 282–285 (2008). doi: 10.1016/j.cub.2008.01.059; pmid: 18302926
20. A. C. Nocera, E. M. Giménez, M. J. Diez, M. V. Retana, G. Winkler, Krill diel vertical migration in Southern Patagonia. *J. Plankton Res.* **43**, 610–623 (2021). doi: 10.1093/plankt/fbab047
21. S. Halfter, E. L. Cavan, P. Butterworth, K. M. Swadling, P. W. Boyd, "Sinking dead"—How zooplankton carcasses contribute to particulate organic carbon flux in the subantarctic Southern Ocean. *Limnol. Oceanogr.* **67**, 13–25 (2022). doi: 10.1002/lno.11971
22. S. A. Henson *et al*., Uncertain response of ocean biological carbon export in a changing world. *Nat. Geosci.* **15**, 248–254 (2022). doi: 10.1038/s41561-022-00927-0
23. T. Rohr, A. J. Richardson, A. Lenton, M. A. Chamberlain, E. H. Shadwick, Zooplankton grazing is the largest source of uncertainty for marine carbon cycling in CMIP6 models. *Commun. Earth Environ.* **4**, 212 (2023). doi: 10.1038/s43247-023-00871-w
24. L. Ratnarajah *et al*., Monitoring and modelling marine zooplankton in a changing climate. *Nat. Commun.* **14**, 564 (2023). doi: 10.1038/s41467-023-36241-5; pmid: 36732509
25. M. Nowicki, T. DeVries, D. A. Siegel, Quantifying the Carbon Export and Sequestration Pathways of the Ocean's Biological Carbon Pump. *Global Biogeochem. Cycles* **36**, e2021GB007083 (2022). doi: 10.1029/2021GB007083
26. T. A. Klevjer *et al*., Large scale patterns in vertical distribution and behaviour of mesopelagic scattering layers. *Sci. Rep.* **6**, 19873 (2016). doi: 10.1038/srep19873; pmid: 26813333
27. B. Cisewski, V. H. Strass, M. Rhein, S. Krägefsky, Raw data of SCADCP (self-contained Acoustic Doppler Current Profiler) from mooring AWI229-6 [dataset]. In supplement to: Cisewski, B et al. (2010): Seasonal variations of diel vertical migration of zooplankton from ADCP backscatter time series data in the Lazarev Sea, Antarctica. Deep Sea Research Part I: Oceanographic Research Papers, 57(1), 78-94. *PANGAEA* (2010).
28. T. Pauly, S. Nicol, I. Higginbottom, G. Hosie, J. Kitchener, Distribution and abundance of Antarctic krill (*Euphausia superba*) off East Antarctica (80–150°E) during the Austral summer of 1995/1996. *Deep Sea Res. Part II Top. Stud. Oceanogr.* **47**, 2465–2488 (2000). doi: 10.1016/S0967-0645(00)00032-1
29. B. Cisewski, V. H. Strass, M. Rhein, S. Krägefsky, Seasonal variation of diel vertical migration of zooplankton from ADCP backscatter time series data in the Lazarev Sea, Antarctica. *Deep Sea Res. Part I Oceanogr. Res. Pap.* **57**, 78–94 (2010). doi: 10.1016/j.dsr.2009.10.005
30. K. Taki, T. Hayashi, M. Naganobu, Characteristics of seasonal variation in diurnal vertical migration and aggregation of Antarctic krill (*Euphausia superba*) in the Scotia Sea, using Japanese fishery data. *CCAMLR Sci.* **12**, 163–172 (2005).
31. G. A. Tarling *et al*., Varying depth and swarm dimensions of open-ocean Antarctic krill *Euphausia superba* Dana, 1850 (Euphausiacea) over diel cycles. *J. Crustac. Biol.* **38**, 716–727 (2018). doi: 10.1093/jcbiol/ruy040
32. M. J. Cox *et al*., Two scales of distribution and biomass of Antarctic krill (*Euphausia superba*) in the eastern sector of the CCAMLR Division 58.4.2 (55°E to 80°E). *PLOS ONE* **17**, e0271078 (2022). doi: 10.1371/journal.pone.0271078; pmid: 36001623
33. I. Everson, Variations in vertical distribution and density of krill swarms in the vicinity of South Georgia. *Mem. Natl. Inst. Polar Res. Spec. Issue* **27**, 84–92 (1983).
34. M. Zhou, R. D. Dorland, Aggregation and vertical migration behavior of *Euphausia superba*. *Deep Sea Res. Part II Top. Stud. Oceanogr.* **51**, 2119–2137 (2004). doi: 10.1016/j.dsr2.2004.07.009
35. Integrated Marine Observing System, IMOS - Argo Profiles - biogeochemical data [Dataset] (2024). https://portal.aodn.org.au/search?uuid=2223b7f2-4bac-4ff1-9b1e-aae9ac58deef.
36. Argo, Argo float data and metadata from Global Data Assembly Centre (Argo GDAC), SEANOE (2000). https://doi.org/10.17882/42182.
37. N.-C. Pauli *et al*., Krill and salp faecal pellets contribute equally to the carbon flux at the Antarctic Peninsula. *Nat. Commun.* **12**, 7168 (2021). doi: 10.1038/s41467-021-27436-9; pmid: 34887407
38. R. Perissinotto, E. A. Pakhomov, C. D. McQuaid, P. W. Froneman, In situ grazing rates and daily ration of

Antarctic krill *Euphausia superba* feeding on phytoplankton at the Antarctic Polar Front and the Marginal Ice Zone. *Mar. Ecol. Prog. Ser.* **160**, 77–91 (1997). doi: 10.3354/meps160077
39. E. A. Pakhomov, R. Perissinotto, P. W. Froneman, D. G. M. Miller, Energetics and feeding dynamics of *Euphausia superba* in the South Georgia region during the summer of 1994. *J. Plankton Res.* **19**, 399–423 (1997). doi: 10.1093/plankt/19.4.399
40. A. Atkinson, K. Schmidt, S. Fielding, S. Kawaguchi, P. A. Geissler, Variable food absorption by Antarctic krill: Relationships between diet, egestion rate and the composition and sinking rates of their fecal pellets. *Deep Sea Res. Part II Top. Stud. Oceanogr.* **59–60**, 147–158 (2012). doi: 10.1016/j.dsr2.2011.06.008
41. E. L. Cavan, S. Kawaguchi, P. W. Boyd, Implications for the mesopelagic microbial gardening hypothesis as determined by experimental fragmentation of Antarctic krill fecal pellets. *Ecol. Evol.* **11**, 1023–1036 (2020). doi: 10.1002/ece3.7119; pmid: 33520184
42. G. A. Tarling, M. L. Johnson, Satiation gives krill that sinking feeling. *Curr. Biol.* **16**, R83–R84 (2006). doi: 10.1016/j.cub.2006.01.044; pmid: 16461267
43. E. L. Cavan *et al*., Antarctic krill sequester similar amounts of carbon to key coastal blue carbon habitats. *Nat. Commun.* **15**, 7842 (2024). doi: 10.1038/s41467-024-52135-6; pmid: 39244635
44. K. M. Archibald, D. A. Siegel, S. C. Doney, Modeling the Impact of Zooplankton Diel Vertical Migration on the Carbon Export Flux of the Biological Pump. *Global Biogeochem. Cycles* **33**, 181–199 (2019). doi: 10.1029/2018GB005983
45. B. A. Krafft *et al*., Standing stock of Antarctic krill (*Euphausia superba* Dana, 1850) (Euphausiacea) in the Southwest Atlantic sector of the Southern Ocean, 2018–19. *J. Crustac. Biol.* **41**, ruab046 (2021). doi: 10.1093/jcbiol/ruab071
46. C. S. Reiss *et al*., Overwinter habitat selection by Antarctic krill under varying sea-ice conditions: Implications for top predators and fishery management. *Mar. Ecol. Prog. Ser.* **568**, 1–16 (2017). doi: 10.3354/meps12099
47. S. Ruiz-Halpern *et al*., Antarctic krill as a source of dissolved organic carbon to the Antarctic ecosystem. *Limnol. Oceanogr.* **56**, 521–528 (2011). doi: 10.4319/lo.2011.56.2.0521
48. B. Meyer, The overwintering of Antarctic krill, *Euphausia superba*, from an ecophysiological perspective. *Polar Biol.* **35**, 15–37 (2012). doi: 10.1007/s00300-011-1120-0
49. T. E. Ryan, R. A. Downie, R. J. Kloser, G. Keith, Reducing bias due to noise and attenuation in open-ocean echo integration data. *ICES J. Mar. Sci.* **72**, 2482–2493 (2015). doi: 10.1093/icesjms/fsv121
50. A. De Robertis, I. Higginbottom, A post-processing technique to estimate the signal-to-noise ratio and remove echosounder background noise. *ICES J. Mar. Sci.* **64**, 1282–1291 (2007). doi: 10.1093/icesjms/fsm112
51. F. Bairstow *et al*., Improving the Accuracy of Krill Target Strength Using a Shape Catalog. *Front. Mar. Sci.* **8**, 658384 (2021). doi: 10.3389/fmars.2021.658384
52. Scientific Committee on Antarctic Research, Southern Ocean Diet and Energetics Database, Zenodo (2023). https://doi.org/10.5281/zenodo.7796465.
53. D. N. Maclennan, P. G. Fernandes, J. Dalen, A consistent approach to definitions and symbols in fisheries acoustics. *ICES J. Mar. Sci.* **59**, 365–369 (2002). doi: 10.1006/jmsc.2001.1158
54. A. J. R. Smith, S. J. Wotherspoon, M. J. Cox, Per-length biomass estimates of Antarctic krill (*Euphausia superba*). *Front. Mar. Sci.* **10**, 1107567 (2023). doi: 10.3389/fmars.2023.1107567
55. M. D. Ohman, J.-B. Romagnan, Nonlinear effects of body size and optical attenuation on Diel Vertical Migration by zooplankton. *Limnol. Oceanogr.* **61**, 765–770 (2016). doi: 10.1002/lno.10251
56. M. D. Ohman, J. A. Runge, E. G. Durbin, D. B. Field, B. Niehoff, On birth and death in the sea. *Hydrobiologia* **480**, 55–68 (2002). doi: 10.1023/A:1021228900786
57. D. J. Morris, I. Everson, C. Ricketts, P. Wards, Feeding of krill around South Georgia. II. Relations between feeding activity, environment and vertical distribution. *Mar. Ecol. Prog. Ser.* **20**, 203–206 (1984). doi: 10.3354/meps020203
58. A. J. R. Smith *et al*., Antarctic krill vertical migrations modulate seasonal carbon export [Dataset], Dryad (2024). https://doi.org/10.5061/dryad.zcrjdfnp3.
59. H. J. Price, K. R. Boyd, C. M. Boyd, Omnivorous feeding behavior of the Antarctic krill *Euphausia superba*. *Mar. Biol.* **97**, 67–77 (1988). doi: 10.1007/BF00391246
60. A. Clarke, L. B. Quetin, R. M. Ross, Laboratory and field estimates of the rate of faecal pellet production by Antarctic krill, *Euphausia superba*. *Mar. Biol.* **98**, 557–563 (1988). doi: 10.1007/BF00391547
61. J. H. Martin, G. A. Knauer, D. M. Karl, W. W. Broenkow, VERTEX: Carbon cycling in the northeast Pacific. *Deep-Sea Res. A, Oceanogr. Res. Pap.* **34**, 267–285 (1987). doi: 10.1016/0198-0149(87)90086-0
62. A. Belcher *et al*., The potential role of Antarctic krill faecal pellets in efficient carbon export at the marginal ice zone of the South Orkney Islands in spring. *Polar Biol.* **40**, 2001–2013 (2017). doi: 10.1007/s00300-017-2118-z; pmid: 32009725
63. F. Planchon *et al*., Carbon export in the naturally iron-fertilized Kerguelen area of the Southern Ocean based on the ^{234}Th approach. *Biogeosciences* **12**, 3831–3848 (2015). doi: 10.5194/bg-12-3831-2015
64. E. Hofmann, C. Lascara, Modeling the growth dynamics of Antarctic krill *Euphausia superba*. *Mar. Ecol. Prog. Ser.* **194**, 219–231 (2000). doi: 10.3354/meps194219
65. A. Belcher *et al*., Krill faecal pellets drive hidden pulses of particulate organic carbon in the marginal ice zone. *Nat. Commun.* **10**, 889 (2019). doi: 10.1038/s41467-019-08847-1; pmid: 30792498
66. E. A. Pakhomov, P. W. Froneman, R. Perissinotto, Salp/krill interactions in the Southern Ocean: Spatial segregation and implications for the carbon flux. *Deep Sea Res. Part II Top. Stud. Oceanogr.* **49**, 1881–1907 (2002). doi: 10.1016/S0967-0645(02)00017-6
67. L. Calise, G. Skaret, Sensitivity investigation of the SDWBA Antarctic krill target strength model to fatness, material contrasts and orientation. *CCAMLR Sci.* **18**, 97–122 (2011).

ACKNOWLEDGMENTS

We are grateful to A. Terauds and P. Boyd for their comments on the manuscript, as well as K. Baker and T. Rohr for helpful discussions in the development of the model. We are indebted to those involved in deploying and retrieving the KOMBI moorings. This project was supported and funded by Australian Antarctic Program Project 4512 and received grant funding from the Australian government as part of the Antarctic Science Collaboration Initiative program. This project also received financial support from Pew Charitable Trust and Antarctic Science Foundation. We acknowledge the use of the CSIRO Marine National Facility (https://ror.org/01mae9353) and grant of sea time on RV *Investigator* in undertaking this research. **Funding:** Australian Antarctic Program Project 4512; Australian government through the Antarctic Science Collaboration Initiative program; Pew Charitable Trust; and Antarctic Science Foundation. **Author contributions:** Conceptualization: A.J.R.S. Data analysis: A.J.R.S., G.R.C., G.J.M., B.H., R.K., S.K., M.J.C. Methodology: A.J.R.S., S.W., L.R., S.K. Writing – original draft: A.J.R.S., S.W., L.R., G.R.C., G.J.M., B.H., R.K., S.K., M.J.C. Writing – review and editing: A.J.R.S., S.W., L.R., G.R.C., G.J.M., B.H., R.K., S.K., M.J.C. **Competing interests:** The authors declare that they have no competing interests. **Data and materials availability:** All data and code generated during this study is publicly available and can be accessed at (*58*). Fluorescence data were collected and made freely available by the International Argo Program and the national programs that contribute to it (https://www.argo.ucsd.edu, https://www.ocean-ops.org/). The Argo Program is part of the Global Ocean Observing System. Argo data were sourced from Australia's Integrated Marine Observing System (IMOS), which is enabled by the National Collaborative Research Infrastructure strategy (NCRIS). IMOS is operated by a consortium of institutions as an unincorporated joint venture, with the University of Tasmania as Lead Agent, with contributions from CSIRO Oceans and Atmosphere, Marine National Facility (MNF), and Curtin University.

SUPPLEMENTARY MATERIALS

science.org/doi/10.1126/science.adq5564
Supplementary Text
Figs. S1 to S8
Table S1
References (*68*–*78*)
MDAR Reproducibility Checklist
Movie S1

Submitted 30 May 2024; resubmitted 20 August 2024
Accepted 5 November 2024
10.1126/science.adq5564